Long-time dynamics of modulated waves in a nonlinear discrete *LC* transmission line

David Yemélé,* Patrick Marquié, and Jean Marie Bilbault
LE2I, FRE CNRS 2309, Université de Bourgogne, Boîte Postale 47870, 21078 Dijon Cedex, France
(Received 29 April 2002; published 14 July 2003)

The long-time dynamics of modulated waves in a nonlinear *LC* transmission line is investigated. Considering the higher-order nonlinear Schrödinger equation, we define analytically the conditions leading to the instability of modulated waves. We show that two kinds of instabilities may develop in the network depending on the frequency range of the chosen carrier wave and on the magnitude of its initial amplitude, which is confirmed by our numerical simulations. The nonreproducibility of numerical experiments on modulated waves is also considered.

DOI: 10.1103/PhysRevE.68.016605 PACS number(s): 41.20.−q

I. INTRODUCTION

In the past few decades, wave propagation in dispersive nonlinear media has received a great amount of attention. This attention is motivated by the capacity of these media to support solitons such as excitations (kinks, pulses, envelope, and dark solitons, etc.) [1,2]. Unlike the other solitons (kinks), envelope solitons require practically no activation energy and can interpolate between extremely nonlinear modes (kinks) and linear modes (linear plane waves). An envelope soliton can be viewed as a result of an instability that leads to a self-induced modulation of the steady state produced by the interaction between nonlinear and dispersive effects. This phenomenon is known as modulational instability (MI). More specifically, modulational instability is a phenomenon in which a continuous wave propagating in a nonlinear medium undergoes, in the presence of weak noise or any other small perturbation, a modulation of its amplitude or phase, which can ultimately end up in breaking up the wave into small packets. This phenomenon has been studied in diverse fields such as fluid dynamics [3], nonlinear optics [4,5], plasma physics [6,7], and nonlinear electrical transmission lines (NLTLs) [8–11]. Indeed, NLTLs are convenient tools to study wave propagation in nonlinear dispersive media. In particular, they provide a useful way to check how the nonlinear excitations behave inside the nonlinear medium and to model the exotic properties of new systems [1,12]. These are the reasons why since the pioneering works by Hirota and Suzuki [13] and by Nagashima and Amagishi [14], on electrical lines simulating the Toda lattice [15], a growing interest has been devoted to the use of NLTLs, in particular, for studying nonlinear modulated wave propagation [8–11,16–18].

The nonlinear Schrödinger (NLS) equation has been shown to provide an approximate but fairly accurate description of such modulated waves in nonlinear media for certain parameter regimes. Indeed, for example, in the field of fluid dynamics, the standard NLS equation gives a good description of nonlinear deep water waves in the case of small steepness, while it fails when considering large steepness. In the latter case, a significant improvement can be achieved by taking into account higher-order terms in perturbation analysis, that is, considering a higher-order NLS (HONLS) equation [19]. More recently, by means of this HONLS equation, Ablowitz and co-workers [20,21] have studied the long-time dynamics of modulational instability of deep water waves and have obtained the following results:

(i) The standard NLS equation yields satisfactory description of long-time envelope solitons dynamics for considered time scales.

(ii) On the contrary, for modulated periodic Stoke waves, serious nonlinear instabilities and chaos may develop in the medium such that the standard NLS equation fails to describe, but which can be explained by means of the HONLS equation.

One might wonder if an intrinsically *discrete medium*, such as an electrical transmission line, may exhibit the same kind of instabilities or chaos as in the above described continuous medium. The answer of this question is the main objective of the present work.

The paper is organized as follows. In Sec. II, we present the characteristics of the NLTL under consideration. In the low-amplitude limit, we derive the HONLS equation governing the propagation of slowly modulated waves in the network. In Sec. III, considering the HONLS equation, we determine the conditions under which a slowly modulated wave propagating along the NLTL will become unstable to a small perturbation. In Sec. IV, in the frequency range where the network may exhibit the propagation of envelope solitons, we use the time-dependent perturbation method to study quantitatively the dynamics of the single envelope soliton. Numerical experiments are considered in Sec. V in order to check the validity of the theoretical predictions and to observe some additional features of modulational instability, namely, the nonreproducibility of numerical experiments. Finally, in Sec. VI, we give some concluding remarks.

II. MODEL DESCRIPTION AND HIGHER-ORDER NONLINEAR SCHRÖDINGER EQUATION

We consider a discrete nonlinear electrical network with N cells, as illustrated in Fig. 1, each cell containing a linear inductance L in the series branch and a nonlinear capacitor in

*Permanent address: Département de Physique, Faculté des Sciences, Université de Dschang, Boîte Postale 067 Dschang, Cameroun. Email address: dyemele@yahoo.fr

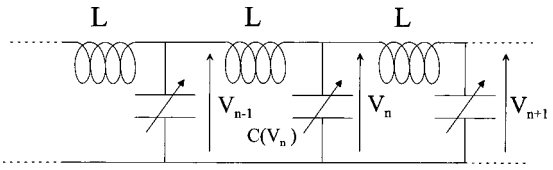

FIG. 1. Electrical network consisting of N identical cells. Each cell contains a linear inductor L in the series branch and a nonlinear capacitor $C(V_n)$.

the shunt branch. Denoting $V_n(t)$ as the voltage across the nth capacitor and using Kirchhoff's laws, we get the circuit equations

$$L\frac{d^2q_n}{dt^2}=V_{n+1}-2V_n+V_{n-1}, \tag{2.1}$$

where q_n is the electrical charge stored in the nth capacitor. This capacitor consists of a reverse-biased diode with differential capacitance $C\ (V_b+V_n)=dq_n/dV_n$, which is a nonlinear function of the voltage V_n. For low voltages around the dc bias voltage V_b, the dependence of $q_n(V_n)$ can be approximated by

$$q_n(V_n)\approx C_0\ \ (V_n-\alpha V_n^2+\beta V_n^3), \tag{2.2}$$

with $C_0=C(V_b)$ and where the nonlinear coefficients α and β are $\alpha=0.21\ \mathrm{V}^{-1}$ and $\beta=0.0197\ \mathrm{V}^{-2}$, respectively, for $V_b=2$ V [1]. By inserting Eq. (2.2) into Eq. (2.1), we obtain the following equations governing wave propagation in the nonlinear network:

$$\frac{d^2V_n}{dt^2}+\omega_0^2(2V_n-V_{n+1}-V_{n-1})=\alpha\frac{d^2V_n^2}{dt^2}-\beta\frac{d^2V_n^3}{dt^2},$$

$$n=1,2,...,N, \tag{2.3}$$

with $\omega_0^2=1/LC_0$. Linear oscillations in the lattice with angular frequency ω and wave number k are described by the following linear dispersion law, represented in Fig. 2:

$$\omega^2=\omega_c^2\sin^2(k/2), \tag{2.4}$$

where $\omega_c=2\omega_0$ is the cutoff frequency due to the intrinsic discrete character of the lattice.

We now focus our attention on modulated waves with a slowly varying envelope in time and space with regard to a given carrier wave with angular frequency $\omega=\omega_p$ and wave vector $k=k_p$. Then, in order to use the reductive perturbation method in the semidiscrete limit [22,23], we introduce the slow envelope variables $X=\varepsilon(n-\nu_g t)$ and $\tau=\varepsilon^2 t$, where ε is a small parameter and $\nu_g=(\omega_0^2/\omega_p)\sin k_p$ designates the group velocity of linear wave packets. Hence, the solution of Eq. (2.3) is assumed to have the following general form:

$$V_n(t)=\varepsilon(Ae^{i\theta}+A^*e^{-i\theta})+\varepsilon^2\phi+\varepsilon^2(Be^{2i\theta}+B^*e^{-2i\theta}), \tag{2.5}$$

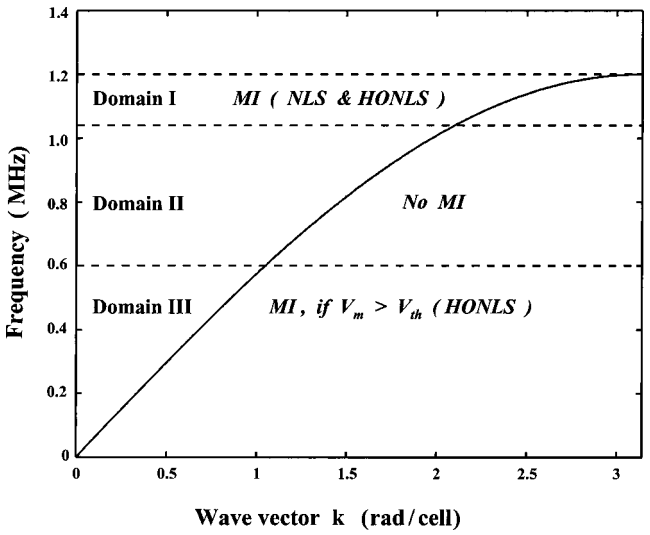

FIG. 2. Linear dispersion curve of the network: frequency $f=\omega/2\pi$ (MHz) as a function of the wave vector k (rad/cell). Three domains are specified: domain I where the network may exhibit MI predicted by the standard NLS equation; domain II where modulated waves are stable; domain III where modulated waves may be unstable if the amplitude of the input carrier wave exceeds a threshold value. This kind of instability is predicted by the HONLS equation, and not by standard NLS equation.

with $\theta=k_pn-\omega_pt$ and $*$ denotes complex conjugation. Note that considering higher-order harmonic terms, that is, terms such as $\exp(\pm 3i\theta),\exp(\pm 4i\theta),...$ is not necessary since all these harmonics lie above the cutoff frequency of our system. So the physical low-pass filter behavior of the electrical line justifies the ansatz (2.5). Substituting Eq. (2.5) in Eq. (2.3) and keeping terms of the order ε^3 and ε^4 proportional to $\exp(i\theta)$, we obtain the following equation for $A(X,\tau)$:

$$i\frac{\partial A}{\partial\tau}+P\frac{\partial^2A}{\partial X^2}+QA|A|^2=\frac{\varepsilon\nu_g}{\omega_p}\left(-\frac{\partial^2A}{\partial X\partial\tau}+i\frac{4}{3}P\frac{\partial^3A}{\partial X^3}+2iQ|A|^2\frac{\partial A}{\partial X}+2iQA^2\frac{\partial A^*}{\partial X}\right), \tag{2.6}$$

with

$$P=-\omega_p/8,\quad Q=\alpha^2\omega_p[(3\beta/2\alpha^2)+(\omega_c/\omega_p)^2-2]. \tag{2.7}$$

Furthermore, the dc and second-harmonic terms $\phi(X,\tau)$ and $B(X,\tau)$, respectively, are related to $A(X,\tau)$ by

$$\phi=2\alpha\ \ [1-(\omega_c/\omega_p)^2]|A|^2,\quad B=\alpha\ \ (\omega_c/\omega_p)^2A^2, \tag{2.8}$$

which have been obtained by keeping the terms proportional to ε^4e^0 and $\varepsilon^2e^{2i\theta}$, respectively. Relations (2.6)–(2.8) are not defined for the carrier frequency $\omega_p=0$; however, since we are concerned with the modulated wave, the carrier frequency cannot reach this limit.

Equation (2.6) governs the propagation of the slowly modulated wave in the NLTL. The first two terms on the right-hand side describe the linear higher-order dispersion, while the two last terms describe the nonlinear dispersion of the network. This equation may be viewed, here and hereafter, as a higher-order NLS (HONLS) equation since it reduces to the standard NLS equation when ε tends to zero, i.e., when neglecting the right-hand terms. In this limit, it is well known that the resulting NLS equation admits different types of soliton solutions depending on the sign of the product of coefficients P and Q. Namely, they are as follows.

(1) If $PQ>0$, the bright-type soliton solution is given by [24]

$$A(X,\tau)=A_0\,\mathrm{sech}[(X-\nu_e P\tau)/L_s]\exp[i(\nu_e/2)(X-\nu_c P\tau)], \tag{2.9}$$

where ν_e and ν_c are the amplitude and phase velocities of the soliton, respectively, and satisfy the following relation $2\nu_e\nu_c=[\nu_e^2-2(Q/P)A_0^2]$, while $L_s=(1/A_0)\sqrt{2P/Q}$ is the spatial width of the soliton.

(2) When $PQ<0$, the solution of the NLS equation is a hole soliton [17,24].

Taking into account the right-hand side of Eq. (2.6), we note that the (HONLS) equation (2.6) modeling the nonlinear modulated wave propagation in the discrete electrical transmission line is very similar to that obtained in the water wave context [20,21], that is, considering a continuous medium. In the following, it is used to determine the conditions of instability of the modulated waves in the network.

III. MODULATIONAL INSTABILITY

In this section, we study the conditions under which a uniform wave train propagating along the NLTL modeled by the HONLS equation (2.6) will become unstable to a small perturbation. For this purpose, we look for a solution of the form

$$A=\rho(X,\tau)e^{ig(X,\tau)}. \tag{3.1}$$

Substituting this relation into Eq. (2.6) leads to an equation in which the real and imaginary parts are respectively given by

$$\begin{aligned}\frac{\partial\rho}{\partial\tau}+2P\frac{\partial g}{\partial X}\frac{\partial\rho}{\partial X}+P\rho\frac{\partial^2 g}{\partial X^2}&=\frac{\varepsilon\nu_g}{\omega_p}\left\{-\left(\frac{\partial g}{\partial\tau}\frac{\partial\rho}{\partial X}+\rho\frac{\partial^2 g}{\partial X\partial\tau}+\frac{\partial g}{\partial X}\frac{\partial\rho}{\partial\tau}\right)+\frac{4P}{3}\left[\frac{\partial^3\rho}{\partial X^3}\right.\right.\\&\left.\left.-3\rho\frac{\partial g}{\partial X}\frac{\partial^2 g}{\partial X^2}-3\left(\frac{\partial g}{\partial X}\right)^2\frac{\partial\rho}{\partial X}\right]+6Q\rho^2\frac{\partial\rho}{\partial X}\right\},\end{aligned}$$

$$\begin{aligned}\frac{\partial g}{\partial\tau}+P\left(\frac{\partial g}{\partial X}\right)^2-Q\rho^2&=\frac{P}{\rho}\frac{\partial^2\rho}{\partial X^2}+\frac{\varepsilon\nu_g}{\omega_p}\left\{\frac{1}{\rho}\frac{\partial^2\rho}{\partial X\partial\tau}-\frac{\partial g}{\partial X}\frac{\partial g}{\partial\tau}\right.\\&+\frac{4P}{3}\left[\frac{3}{\rho}\frac{\partial g}{\partial X}\frac{\partial^2\rho}{\partial X^2}+\frac{3}{\rho}\frac{\partial^2 g}{\partial X^2}\frac{\partial\rho}{\partial X}+\frac{\partial^3 g}{\partial X^3}\right.\\&\left.\left.-\left(\frac{\partial g}{\partial X}\right)^3\right]+2Q\rho^2\frac{\partial g}{\partial X}\right\}.\end{aligned} \tag{3.2}$$

This system of equations has the exact plane wave solution $A=\rho_0 e^{ig_0(\tau)}$, where ρ_0 is a constant amplitude and $g_0(\tau)=2Q\rho_0^2\tau$. It is the well-known continuous wave solution of the NLS equation with a phase or angular frequency depending on the square of the amplitude.

The linear stability of this continuous wave can be investigated by looking for a solution of the form

$$A=[\rho_0+\rho_1(X,\tau)]e^{i[g_0(\tau)+g_1(X,\tau)]}, \tag{3.3}$$

where $\rho_1(X,\tau)$ and $g_1(X,\tau)$ are assumed to be small as compared to the carrier wave parameters ρ_0 and $g_0(\tau)$, respectively. Substituting Eq. (3.3) in Eq. (3.2), and neglecting the nonlinear terms, leads to the following linear equations for ρ_1 and g_1:

$$\begin{aligned}\frac{\partial\rho_1}{\partial\tau}+P\rho_0\frac{\partial^2 g_1}{\partial X^2}&=\frac{\varepsilon\nu_g}{\omega_p}\left\{5Q\rho_0^2\frac{\partial\rho_1}{\partial X}-\rho_0\frac{\partial^2 g_1}{\partial X\partial\tau}+\frac{4P}{3}\frac{\partial^3\rho_1}{\partial X^3}\right\},\\\frac{\partial g_1}{\partial\tau}-2Q\rho_0\rho_1&=\frac{P}{\rho_0}\frac{\partial^2\rho_1}{\partial X^2}+\frac{\varepsilon\nu_g}{\omega_p}\left\{\frac{1}{\rho_0}\frac{\partial^2\rho_1}{\partial X\partial\tau}+Q\rho_0^2\frac{\partial g_1}{\partial X}\right.\\&\left.+\frac{4P}{3}\frac{\partial^3 g_1}{\partial X^3}\right\}.\end{aligned} \tag{3.4}$$

Assuming for the perturbation a modulation ansatz with wave number K and angular frequency Ω, namely, $\rho_1=ae^{i(\Omega\tau-KX)}+\text{c.c.}$ and $g_1=be^{i(\Omega\tau-KX)}+\text{c.c.}$, where a and b are constants and c.c. stands for complex conjugate, leads to the perturbation dispersion law,

$$\begin{aligned}&\Omega^2(1-\zeta^2K^2)-2\zeta K(\tfrac{1}{3}PK^2-2Q\rho_0^2)\Omega-\{P^2K^4\\&\quad-2PQ\rho_0^2K^2-\zeta^2K^2(\tfrac{16}{9}P^2K^4-8PQ\rho_0^2K^2+5Q^2\rho_0^4)\}\\&\quad=0,\end{aligned} \tag{3.5}$$

where $\zeta=\varepsilon\nu_g/\omega_p$. The modulational instability phenomenon occurs when the angular frequency Ω of the perturbation possesses a nonzero imaginary part leading to an exponential growth of the amplitude versus time. This occurs when the discriminant of the homogeneous algebraic equation has a negative value, that is,

$$\Delta=\frac{16}{9}\zeta^4P^2K^2(K^6+c_2K^4+c_1K^2+c_0)<0, \tag{3.6}$$

with $d=\zeta^2(Q/P)\rho_0^2$, $c_0=-(9/16\zeta^6)d(d+2)$, $c_1=(9/16\zeta^4)[1+(26/3)d+5d^2]$, and $c_2=-(3/2\zeta^2)(1+3d)$. This sign of Δ depends on the sign of Q/P and on the amplitude ρ_0 of the carrier wave, given as follows.

(i) Δ is negative for $Q/P>0$ if the wave number K is lower than the critical value K_{c_1} given by

$$K_{c_1}^2=(s_1+s_2)-(c_2/3), \tag{3.7}$$

with

$$s_1=[r+(q^3+r^2)^{1/2}]^{1/3}, \quad s_2=[r-(q^3+r^2)^{1/2}]^{1/3},$$

$$r=\frac{1}{6}(c_1c_2-3c_0)-\frac{c_2^3}{27},$$

and $q=c_1/3-c_2^2/9$.

(ii) Δ is also negative for $Q/P<0$ if the carrier wave amplitude exceeds a threshold

$$\varepsilon\rho_0>\varepsilon\rho_{0,\mathrm{th}}=(\omega/v_g)(-2P/Q)^{1/2} \tag{3.8}$$

and if the wave vector K of the modulation obeys

$$K^2<K_{c2}^2=(-1/2)(s_1+s_2)-c_2/3-i(\sqrt{3}/2)(s_1-s_2). \tag{3.9}$$

Equations (3.7), and (3.8) and (3.9) determine the conditions of instability of slowly modulated plane waves propagating along the NLTL. It appears from Eq. (3.7) that the instability occurs when the product PQ is positive and if the wave vector K of the modulation is lower than K_{c_1}. We find here a result similar to that given by the standard NLS equation, the presence of higher-order terms in Eq. (2.6) implying a slightly modified value of K_{c_1}. In fact, note that for $\varepsilon\rightarrow 0$, the HONLS equation corresponds to the standard NLS equation, and K_{c_1} reduces to the well-known expression $K_{c_1}=\rho_0(2Q/P)^{1/2}$. This result is shown in the dispersion curve (Fig. 2), where the corresponding domain (domain for which $PQ>0$) is labeled by domain I. Another criterion of instability, absent for the standard NLS equation, is given by Eqs. (3.8) and (3.9). In this case, instability may occur, when $PQ<0$, if the wave vector of the modulation is lower than K_{c_2}, and if the carrier wave amplitude exceeds the threshold value $V_{\mathrm{th}}=2\varepsilon\rho_{0\mathrm{th}}$ [see Eqs. 2.5 and (3.1)] depending on the carrier wave frequency and on the characteristic parameters of the NLTL [α, β, and $u_0=(LC_0)^{-1/2}$] via the nonlinear coefficient Q in the HONLS equation. In Fig. 3, the threshold amplitude V_{th} is plotted versus the carrier wave frequency f_p. Let us point out first that V_{th} is bounded by the biased voltage $V_b=2$ V of BB112 varicap diodes.

Then, two regions appear corresponding, respectively, to stable and unstable propagations of slowly modulated waves according to their initial amplitude as compared to the threshold value. For the sake of clarity, these results are also shown in the corresponding region $PQ<0$ of the dispersion curve (Fig. 2), where the following two domains of stability are then specified: Domain II. corresponds to the case where there is no instability for carrier wave amplitude less than V_b, since the threshold value V_{th} exceeds the biased voltage; and Domain III corresponds to the region where instability occurs when the carrier wave amplitude exceeds the threshold value V_{th} that is lower than the biased voltage V_b.

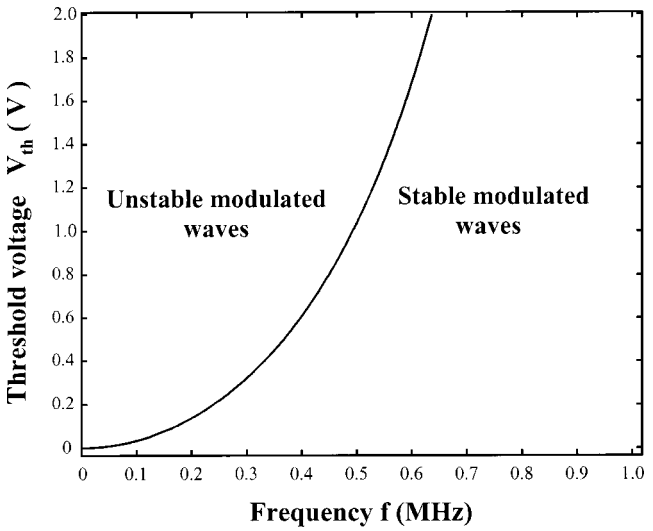

FIG. 3. Threshold value $V_{\mathrm{th}}=2\varepsilon\rho_{0\mathrm{th}}$ (V), as a function of carrier wave frequency, $f_p=\omega_p/2\pi$ (MHz).

It is necessary to point out that our results in the case $PQ<0$ are similar to those obtained by considering other discrete systems, namely, the ϕ^4 model [25] and another type of the NLTL [26]. However, a quantitative comparison of results is not possible since both these models consist of band-pass filters for linear waves, while our model consists of a low-pass filter. Nevertheless, it should be interesting to use the HONLS equation to establish the criterion of instability of slowly modulated plane waves propagating in these other systems in order to make a quantitative comparison.

IV. EFFECT OF HIGHER-ORDER TERMS ON THE ENVELOPE SOLITON DYNAMICS

In the preceding section, our analytical calculations on modulational instability conditions in the NLTL modeled by an HONLS equation have predicted instability for $Q/P>0$ (domain I in Fig. 2), that is, as in the NLS case. This criterion of instability being related to the existence of envelope solitons in this region, the higher-order terms [right-hand side of Eq. (2.6)] can then be viewed as small perturbations to the standard NLS equation. Although the influence of small perturbations in the NLS equations is known to affect the velocity, amplitude, and phase of the envelope solitons and to generate small-amplitude wave packets [27,28], one might wonder how the perturbation terms in the HONLS equation (2.6) will *quantitatively* modify the envelope soliton parameters existing in domain I of the dispersion curve (see Fig. 2).

To proceed with perturbation effects on envelope soliton dynamics, it is more convenient to use dimensionless parameters: $u=(Q/2P)^{1/2}A$, $T=(2P)\tau$, and $x=X$, which leads to the dimensionless form of the HONLS equation

$$i\frac{\partial u}{\partial T}+\frac{1}{2}\frac{\partial^2 u}{\partial X^2}+u|u|^2=i\varepsilon R[u], \tag{4.1a}$$

where

$$R[u]=(\nu_g/\omega_p)\left[i\frac{\partial^2 u}{\partial X\partial T}+\frac{2}{3}\frac{\partial^3 u}{\partial X^3}+4|u|^2\frac{\partial u}{\partial X}+2u^2\frac{\partial u^*}{\partial X}\right] \tag{4.1b}$$

stands for the perturbation. Similarly, the dimensionless form of the unperturbed NLS soliton is given by [see Eq. (2.9)]

$$u_s(z,T)=2a\,\mathrm{sech}\,z\exp(i\Theta), \tag{4.2}$$

with $z=2a[X-\xi(T)]$, $\Theta=(\mu/a)z+\delta(T)$, $\xi(T)=2\mu T$, and $\delta(T)=2(\mu^2+a^2)T$, where 2μ and $2a$ are the dimensionless soliton velocity in the moving frame at velocity ν_g and amplitude, respectively. To describe the variations of the envelope soliton parameters (a, μ, ξ, and δ), let us consider that all these parameters change with time according to the well-known time-dependent perturbation theory [27,28]:

$$\frac{da}{dT}=\varepsilon N[u], \tag{4.3}$$

$$\frac{d\mu}{dT}=\varepsilon M[u],$$

$$\frac{d\xi}{dT}=-\frac{1}{2a}\mathrm{Im}\,h(\chi)+\varepsilon E[u],$$

$$\frac{d\delta}{dT}=2\mu\frac{d\xi}{dT}+\mathrm{Re}\,h(\chi)+\varepsilon D[u],$$

with

$$N[u]=\frac{1}{2}\mathrm{Re}\int_{-\infty}^{+\infty}R[u_s]e^{-i\Theta}\,\mathrm{sech}\,z\,dz,$$

$$M[u]=\frac{1}{2}\mathrm{Im}\int_{-\infty}^{+\infty}R[u_s]e^{-i\Theta}\,\mathrm{sech}\,z\tanh z\,dz,$$

$$h(\chi)=2(a^2-\mu^2)-4i\mu a, \tag{4.4}$$

$$E[u]=\frac{1}{4a^2}\mathrm{Re}\int_{-\infty}^{+\infty}R[u_s]e^{-i\Theta}z\,\mathrm{sech}\,z\,dz,$$

$$D[u]=\frac{1}{2a}\mathrm{Im}\int_{-\infty}^{+\infty}R[u_s]e^{-i\Theta}(1-z\tanh z)\mathrm{sech}\,z\,dz.$$

Replacing Eq. (4.2) in Eq. (4.1b), then integrating, yields

$$da/dT=0,$$

$$d\mu/dT=0,$$

$$d\xi/dT=\frac{2\mu+(10\varepsilon\nu_g/3\omega_p)(3\mu^2-a^2)+32(\varepsilon^2\nu_g^2/3\omega_p^2)\mu(\mu^2-a^2)}{1+4(\varepsilon\nu_g/\omega_p)\mu+4(\varepsilon^2\nu_g^2/\omega_p^2)(\mu^2-a^2)}, \tag{4.5}$$

$$d\delta/dT=\frac{2(\mu^2+a^2)+(16\mu\varepsilon\nu_g/3\omega_p)(a^2+2\mu^2)+32(\varepsilon^2\nu_g^2/3\omega_p^2)(\mu^4+a^2\mu^2-a^4)}{1+4(\varepsilon\nu_g/\omega_p)\mu+4(\varepsilon^2\nu_g^2/\omega_p^2)(\mu^2-a^2)},$$

from which it appears that the amplitude of the soliton is not modified ($da/dT=0$), while the soliton velocity $d\xi/dT$ undergoes a constant deviation because $d\mu/dT=0$. From Eq. (4.5), we can show that the nonlinear frequency of the soliton Ω_ε defined by

$$\Omega_\varepsilon=2\mu\frac{d\xi}{dT}-\frac{d\delta}{dT} \tag{4.6}$$

also undergoes a constant modification, whose explicit expression is

$$\Omega_\varepsilon=\frac{2(\mu^2-a^2)+\frac{4}{3}\frac{\varepsilon\nu_g}{\omega_p}\mu(7\mu^2-9a^2)+\frac{32}{3}\left(\frac{\varepsilon\nu_g}{\omega_p}\right)^2(\mu^4-3a^2\mu^2+2a^4)}{1+4\frac{\varepsilon\nu_g}{\omega_p}\mu+4\left(\frac{\varepsilon\nu_g}{\omega_p}\right)^2(\mu^2-a^2)}. \tag{4.7}$$

For example, in the case of an electrical soliton propagating at the group velocity ν_g in the network (which corresponds to $\mu=0$), the deviation of the nonlinear frequency is given by

$$\Delta\Omega=\Omega_\varepsilon-\Omega_{\varepsilon=0}=(80P/3)(\nu_g/\omega_p)^2(\varepsilon a)^4/[1-4(\varepsilon\nu_g/\omega_p)^2a^2]. \tag{4.8}$$

The consequence of this deviation will be observed in the numerical experiments presented in the following section.

V. NUMERICAL EXPERIMENTS

In this section, we present the details and the results of numerical experiments performed on the nonlinear electrical network. We first consider the experiments with slowly

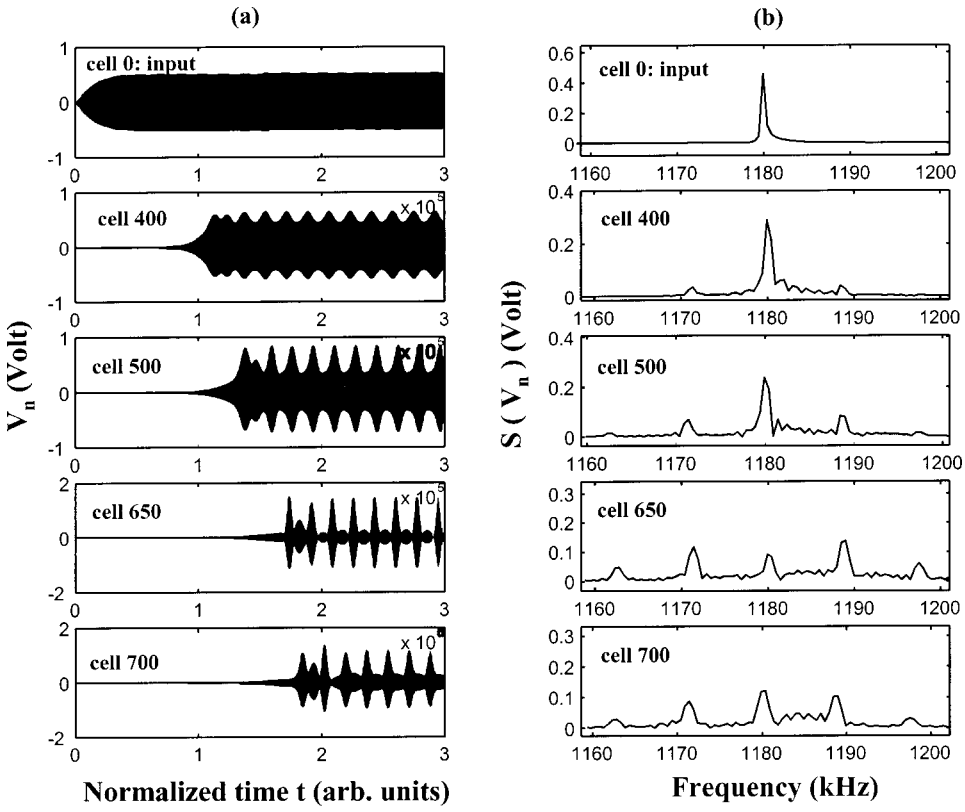

FIG. 4. Signal voltage (in volts) as a function of normalized time (arbitrary units) (a) and corresponding power spectrum (in volts) (b), showing MI of a slowly modulated plane wave, at frequency $f_p = 1180$ kHz belonging to domain I of the dispersion curve, predicted by the NLS and HONLS equations. The initial amplitude of the wave is $V_m = 0.5$ V, while the modulation rate and the modulation frequency are $m = 0.01$ and $f_m = 8.75$ kHz, respectively.

modulated plane waves and then experiments on envelope soliton propagation are presented.

A. Modulated plane waves

According to the analytical calculations presented in Sec. III, the stability of modulated plane waves is determined by the sign of the parameters P and Q, where P is the dispersion coefficient and Q is the nonlinear coefficient of the standard NLS equation. A slowly modulated plane wave may become unstable when $PQ>0$ and also when $PQ<0$, but in the latter case, the plane wave amplitude has to exceed the critical value $V_{\mathrm{th}} = 2\varepsilon\rho_{0\mathrm{th}}$ (see Fig. 3). However, this stability analysis has been obtained through a linear equation (3.4) which is only an approximative description of the initial equation (3.2). Therefore, the linear stability analysis can only detect the onset of instability, but it does not tell us anything about the behavior of the system when the instability takes place.

In order to check the validity of the analytical predictions of MI presented in Sec. III, we perform numerical simulations of the exact equation (2.3) governing wave propagation in the NLTL. The parameters of the line are chosen to be $L_1 = 220\ \mu$H, $C(V_b = 2\ \mathrm{V}) = C_0 = 320$ pF which implies that the cutoff frequency $f_c = \omega_c/2\pi = 1200$ kHz. The fourth order Runge-Kutta scheme is used with normalized integration time step $\Delta t = 5\times10^{-3}$ corresponding to the sampling period $T_s = 1.33\times10^{-9}$ s. Similarly, the number of cells is variable in order to avoid wave reflection at the end of the line and, also, to run the experiments with sufficiently large time (for example, $t = 4$ ms).

At the input of the line, we apply a slowly modulated signal

$$V_0(t) = V_m(1 + m\cos\Omega t)\cos\omega_p t, \tag{5.1}$$

where V_m is the amplitude of the unperturbed plane wave (carrier wave) with angular frequency $\omega_p = 2\pi f_p$. In addition, m and $\Omega = 2\pi f_m$ are the rate and the angular frequency of the modulation, respectively. We have investigated the stability over the whole carrier wave frequency range $f_p \leqslant f_c$, and for different modulation frequencies 0.1 kHz$\leqslant f_m \leqslant$10 kHz.

For $f_p \in]f_{\mathrm{cr}} = 1040\ \mathrm{kHz}, f_c]$, that is, in domain I of the dispersion curve, where $PQ>0$, instabilities have been detected, as predicted in Sec. III. The above mentioned instability leads to a self-modulation of the wave as represented in Fig. 4. In this figure, the signal voltage at different cells is represented in Fig. 4(a), while the corresponding Fourier spectra are represented in Fig. 4(b). The parameters of the input signal are $V_m = 0.5$ V, $f_p = 1180$ kHz, $f_m = 8.75$ kHz, and $m = 1\%$. As time goes on and as the wave travels along the electrical network, the modulation increases and the continuous wave breaks into a periodic pulse train with amplitude larger than the initial amplitude of the carrier wave. The wave spectrum shows a growth of the modulation (with spectral components $f_{1\pm} = f_p \pm f_m$) and the generation of other frequencies $f_{2\pm} = f_p \pm 2\ f_m$ which may be interpreted by the existence of phase modulation (PM) resulting of a conversion AM (amplitude modulation)-PM [29]. Note that the second harmonic generated by the network is not represented in this figure since its amplitude is very small as com-

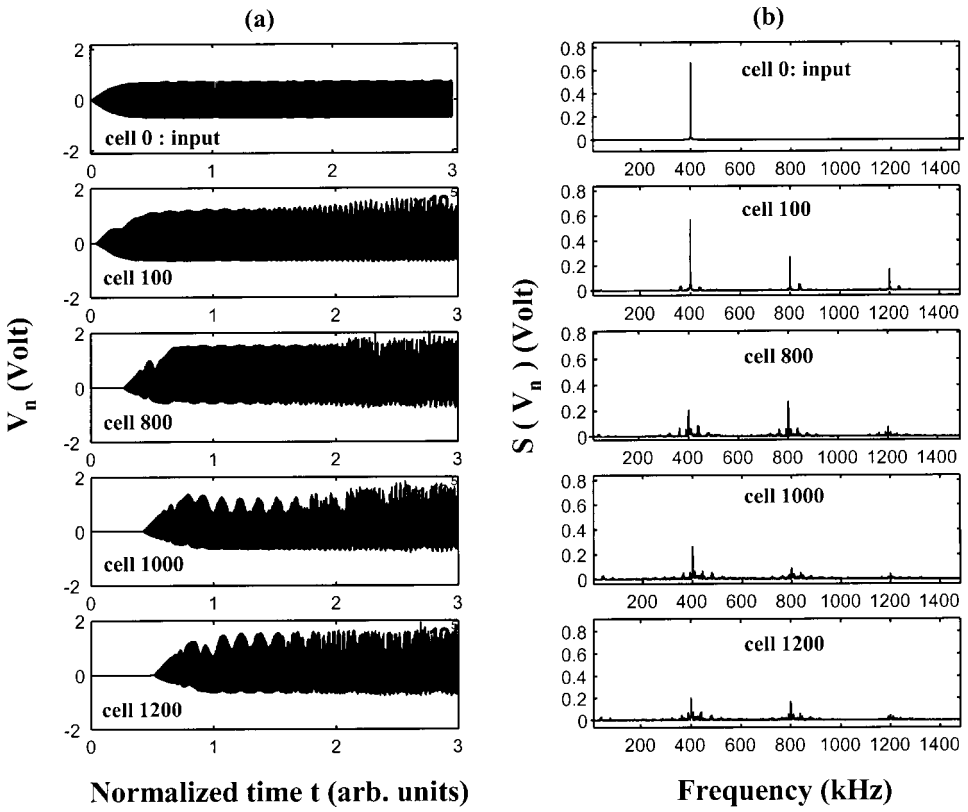

FIG. 5. Signal voltage (in volts) as a function of normalized time (arbitrary units) (a) and corresponding power spectrum (in volts) (b), showing MI of a slowly modulated plane wave, at frequency $f_p = 400$ Khz belonging to domain III of the dispersion curve, predicted only by HONLS equation. The initial amplitude of the wave is $V_m = 0.7\ \mathrm{V} > V_{\mathrm{th}} = 0.5\ \mathrm{V}$, while the modulation rate and the modulation frequency are $m = 0.01$ and $f_m = 8.75$ kHz, respectively.

pared to the amplitude of the fundamental. The existence conditions of this kind of instability are adequately described by the standard NLS equation.

In domain II of the dispersion curve, the numerical simulations have confirmed the stability of propagating modulated plane waves for the allowed values of the initial signal voltage amplitude (less than 2V).

Next, for $f_p \leqslant f_c/2$ corresponding to domain III of the dispersion curve, instabilities develop for some values of the plane wave amplitude exceeding a certain threshold value defined by Eq. (3.8). For example, for $f_p = 400$ kHz, $f_m = 10$ kHz, and $V_m = 0.7\ \mathrm{V} > V_{\mathrm{th}} = 0.5\ \mathrm{V}$, Fig. 5(a) shows the voltage signal versus time for different cells. Here, unlike the instabilities observed in domain I from which a pulse train is generated, this kind of instability leads to an incoherent wave. The number of created frequency components increases as one can easily observe in the Fourier spectrum [Fig. 5(b)], and the electrical network reaches a chaoticlike state. The origin of this kind of instability may be attributed to the important rate of a generated second harmonic as compared to the fundamental term with frequency f_p belonging to domain III, contrary to the case where frequency f_p is chosen in domain I. Note that this interpretation is in accordance with the analytical expression of the second-harmonic term B [Eq. (2.8)], which is more important for low frequencies than for higher frequencies. Therefore, the nonlinear coefficient Q becomes more important in domain III, inducing the generation of multiple spectral components. Finally, we mention that the existence of this kind of MI in domain III can only be predicted by taking into account the presence of the higher-order terms in the HONLS equation (3.6).

This incoherent evolution of modulated plane waves can also be evidenced from the nonreproducibility of experiments devoted to their propagation in the nonlinear medium, as observed by Ablowitz *et al.* [21] in the context of fluid dynamics, that is, considering modulated periodic Stokes waves in deep water. For two different experiments with initial identical signals generated by the wave maker, the resulting temporal evolutions of the surface displacement at a given position in the tank are graphed against each other to produce a ''phase plane'' plot indicating the level of reproducibility. In particular, if the two experiments can be considered to be reproducible near the wave maker, which corresponds to a 45° line in the phase plane, on the contrary, a complex graph is obtained for more distant positions in the tank. This complex graph traduces the nonreproducibility of both experiments and modulated periodic Stokes waves, which is attributed to the development of a phase shift between the waves of the two experiments, this unavoidable phase shift being a function of time. Here, as we consider modulated plane waves in an NLTL, this phase shift is replaced by the existence of a small level of noise present in each cell. Then, in our numerical experiments, a zero mean Gaussian noise with standard deviation $\sigma = 5 \times 10^{-3}$ is added in each cell as an additional initial condition. In the phase plane plots, the evolution of the voltage $V_n^{(1)}(t)$ is graphed against the evolution of the voltage $V_n^{(2)}(t)$, $V_n^{(1)}(t)$, and $V_n^{(2)}(t)$ being the temporal voltages measured at the same cell n, and obtained using the same input signal $V_0(t)$ for two different experiments. For these experiments, we distinguish three cases corresponding to stability domains of the dispersion curve labeled by domains I, II, and III. For all domains, the phase plane plot is a 45° line for the cells

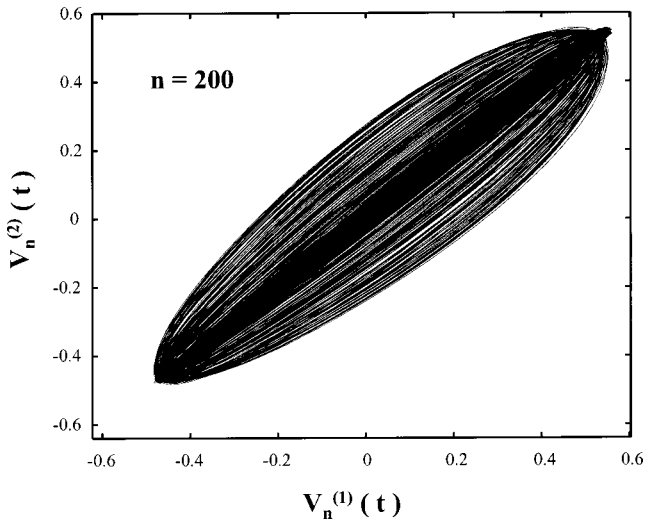

FIG. 6. Phase plane plot $V_n^{(2)}(t)$ vs $V_n^{(1)}(t)$ (in volts) for a slowly modulated wave with parameters: amplitude $V_m=0.5$ V, carrier wave frequency $f_p=1000$ kHz belonging to domain II of the dispersion curve. Frequency modulation $f_m=10$ kHz and modulation rate $m=0.01$.

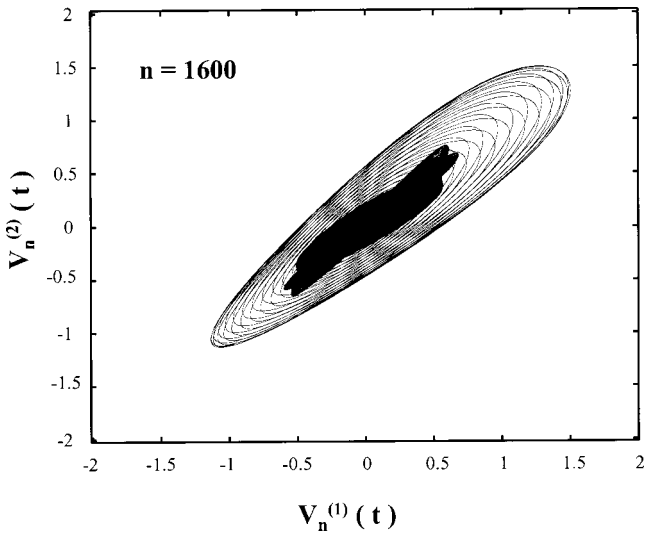

FIG. 7. Phase plane plot $V_n^{(2)}(t)$ vs $V_n^{(1)}(t)$ (in volts) for a slowly modulated wave with parameters: amplitude $V_m=0.5$ V, carrier wave frequency $f_p=1150$ kHz, belonging to domain I of the dispersion curve. Frequency modulation $f_m=10$ kHz and modulation rate $m=1\%$.

near the input cell, and spreads when the wave propagates along the network, i.e., for more distant cells. In this case, the two experiments diverge from each other, indicating that the experiments are nonreproducible. Furthermore, the geometry of the graph traduces the dynamics of nonlinear modulated waves, behaving from pseudocoherent to chaoticlike state, depending on the choice of the carrier frequency f_p. Indeed, for $f_p=1000$ kHz chosen in domain II, where no MI was predicted, the phase plane plot at cell 200 (represented in Fig. 6) shows a quite coherent structure materializing the stability of the waves. Next, the plot obtained for $f_p=1150$ kHz in domain I where MI exists at cell 1600 exhibits a noncoherent structure (see Fig. 7). Finally, the completely chaoticlike state graph obtained in domain III (see Fig. 8), with $f_p=400$ kHz, traduces the particular instability of modulated waves observed in this frequency range and previously described. Furthermore, a quasirecurrence instability phenomenon with 50 cells recurrence length is observed since, as shown in Fig. 8, the phase plane plots related to cells 100 and 150, and cells 130 and 180, respectively, are very similar. Let us point out that the same 50 cells recurrence length was also observed when launching a nonmodulated wave with the same frequency in the NLTL, this phenomenon being closely connected to the intrinsic discrete character of the medium.

B. Electrical envelope solitons

In this paragraph, the effects of higher-order terms in the HONLS equation will be considered, while studying numerically the propagation of the N-bound envelope solitons that may exist in domain I of the dispersion curve (Fig. 2). As an initial condition for the numerical experiment, we consider the input signal

$$V_0(t)=N_s V_m \,\mathrm{sech}(\nu_g t/L_s)\cos(\omega_p t), \qquad (5.2)$$

where $L_s=(2/V_m)\sqrt{2P/Q}$ and N_s are the soliton width and the number of bound solitons, respectively. We chose as a specific case $N_s=3$ and a carrier wave frequency belonging to domain I, $f_p=1150$ Khz, which corresponds to the group velocity $\nu_g=1073$ cells/ms. In addition, the soliton amplitude $V_m=0.35$ V implies $L_s=19$ cells.

As presented in Fig. 9, the fission of the initial three bound solitons is observed at cells 0, 2000, 4000, and 8000, respectively, which justifies the description of the modulated wave dynamics in the NLTL by the HONLS equation (2.6). This fission, which is attributed to the higher-order terms in HONLS equation, generates three solitons whose amplitudes $5V_m$, $3V_m$, and V_m exactly correspond to the predicted one, from inverse scattering calculations (see Ref. [24], and references therein).

To understand these experiment results, one might construct the two first lowest quantities of the conservation law of the NLS equation, that is, $C_1=\int_{-\infty}^{+\infty}|u|^2dX$ and $C_2=\int_{-\infty}^{+\infty}(u^*(\partial u/\partial X)-u(\partial u^*/\partial X))dX$, where C_1 and C_2 may be viewed as the soliton energy and the soliton momentum, respectively, and where u verifies the dimensionless HONLS equation (4.1). Both quantities are conserved if the higher-order terms are neglected. Indeed, the N number of solitons solution of the NLS equation supplied as an input wave propagate at exactly the same speed and the resulting envelope shape oscillates due to the phase interference among the solitons [30].

However, in the presence of the higher-order terms present in the HONLS equation (2.6), the momentum C_2 is modified while the soliton energy C_1 is still conserved, that is, $dC_1/dT=0$ and $dC_2/dT\neq 0$. Because of this modification (decreasing), which depends on soliton parameters [see relations (4.5) and (4.7)], the N-bound solitons propagate at different speeds due to their different amplitudes and hence, they separate (see Fig. 9). A similar result has been already

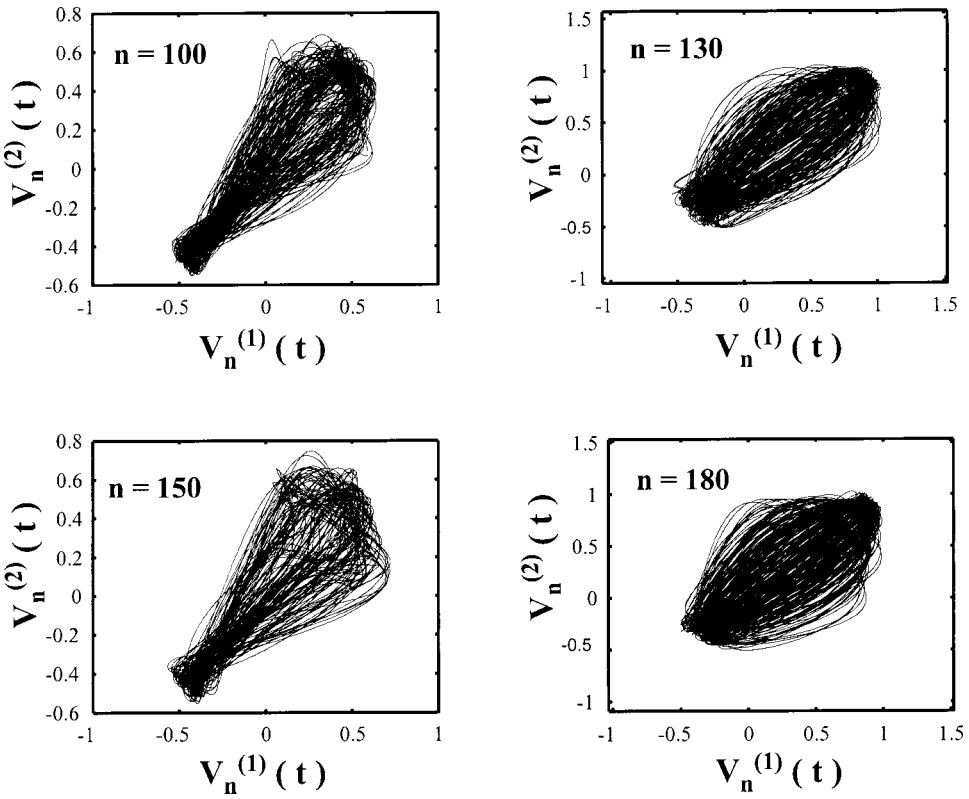

FIG. 8. Phase plane plots $V_n^{(2)}(t)$ vs $V_n^{(1)}(t)$ (in volts) for a slowly modulated wave with parameters: amplitude $V_m = 0.5$ V, carrier wave frequency $f_p = 400$ kHz belonging to domain III of the dispersion curve. Frequency modulation $f_m = 10$ kHz and modulation rate $m = 1\%$.

obtained in the context of nonlinear optics [31–33] where similar higher-order terms to the NLS equation describing the propagation of pulse soliton in the optical fiber were derived [30]. Among the three additional terms in the HONLS equation, that is, the linear higher dispersion term, the nonlinear dispersion term, and the self-induced Raman effect, the last term that produces the downshift of the nonlinear frequency of the soliton was shown to play the most

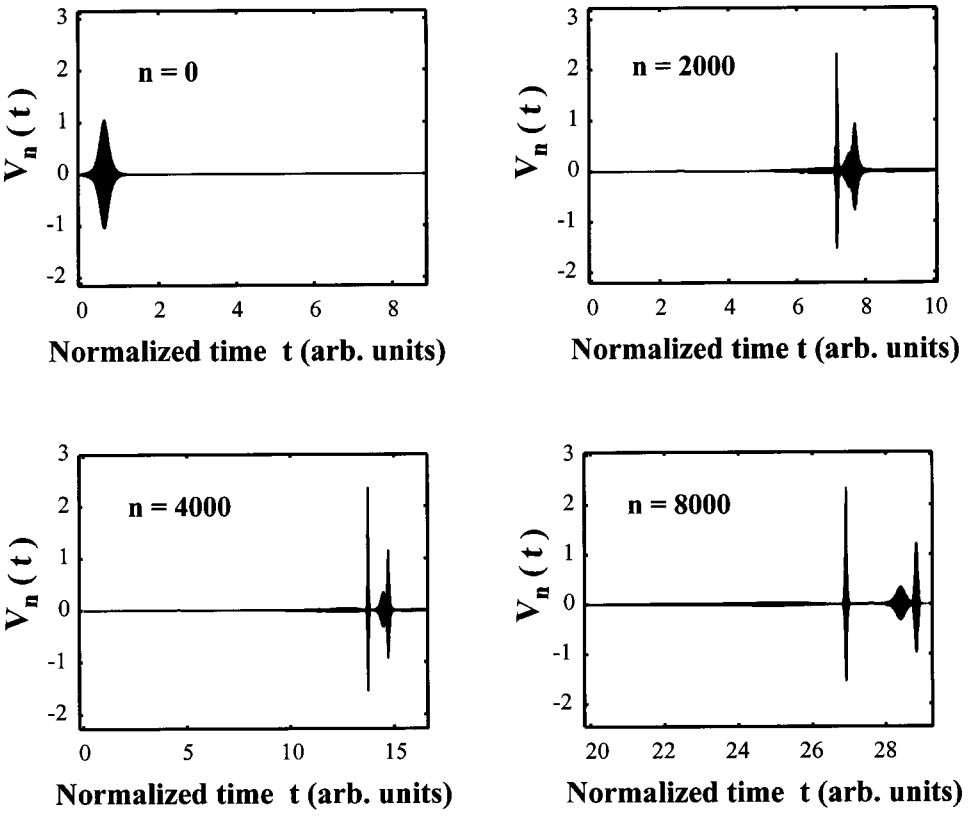

FIG. 9. Plot of signal voltage (in volts) as a function of normalized time (arbitrary units) showing the propagation and the fission of three-bound solitons of amplitude $3V_m$ (with $V_m = 0.35$ V) because of the presence of higher-order terms with respect to the standard NLS equation. The soliton of amplitude $5V_m$ is first ejected at cell 2000, while the later are ejected at cell 8000.

dominant role [24,34]. However, the Raman effect is more manifested since it gives a constant deceleration inducing the increase of the soliton velocity with respect to the propagation distance.

Finally, as considered previously in the study devoted to modulated plane waves MI, one might wonder whether the experiments on soliton propagation are reproducible or not. Then numerical experiments were run considering for an initial condition an input signal obeying Eq. (5.2) with $N_s=1$ (single soliton), and a small level of noise in each cell (see Sec. V B for the noise parameters). The phase plane plots (not presented here) presenting the experimental results show a nearly perfect 45° line indicating the reproducibility of experiments on envelope solitons in the NLTL, as observed by Ablowitz *et al.* [21] in their experiments in the hydrodynamics tank.

VI. CONCLUSION

In this paper, we have investigated the long-time dynamics of modulated waves in a nonlinear discrete electrical transmission line by considering additional higher-order terms to the standard NLS equation. First, we have shown that the resulting HONLS equation allows to predict different features concerning the stability of a slowly modulated wave. In the standard NLS domain of the MI corresponding to $PQ>0$, the perturbations of low-amplitude carrier waves provide an instability leading ultimately in the breaking up of the wave into envelope solitons. In fact, in this frequency domain, the additional terms to the NLS equation do not *qualitatively* modify the results obtained with the standard NLS equation. More interestingly, and contrary to the NLS case, for a negative value of the product PQ, additional terms are at the origin of the instability of carrier waves against all possible perturbations, provided that their initial amplitude is greater than a particular threshold. These predictions are confirmed by numerical simulations. Furthermore, and contrary to the NLS-type MI, the instability observed for $PQ<0$ does not lead to the generation of envelope solitons since a chaoticlike state is reached. Note that it would be now interesting to characterize this chaoticlike behavior with appropriate tools such as Poincaré sections, Lyapunaov exponents, etc.

Next, we have investigated the effects of higher-order terms on the envelope soliton propagation (in their domain of existence, i.e., $PQ>0$) using a perturbative analysis. We have shown that the higher-order terms have no effect on the amplitude of the soliton, while they modify its nonlinear frequency. Consequently, this nonlinear frequency downshift may produce the fission of N-bound solitons propagating in the lattice, as observed in our numerical experiments.

Finally, this study on the dynamics of modulated waves in the NLTL has been completed by results on experiments of the reproducibility devoted to the propagation of both modulated plane waves and envelope solitons. Considering two different experiments with the same identical conditions, the phase plane plot obtained with the two results present a 45° line in the case of envelope solitons, transducing a stable evolution adequately described by the NLS equation [21]. On the contrary, numerical experiments on modulated plane waves are not reproducible since the phase plane plot strongly differs from a 45° line, particularly in the domain where the MI occurs due to higher-order terms to the NLS equation. Indeed, the graphs obtained in this case present a chaoticlike structure. This reproducibility of soliton and irreproducibility of modulated plane wave experiments observed here in a discrete electrical transmission line bear comparison with the experimental results obtained by Ablowitz *et al.* [21] in the water wave context, that is, considering a continuous medium. This allows us to conclude that the phenomenon (nonreproducibility) may exist in several physical systems modeled by an NLS equation at a leading order, this equation being only an approximate equation governing the propagation of modulated waves in nonlinear dispersive media.

ACKNOWLEDGMENT

One of the authors, D.Y. would like to acknowledge The Conseil Régional de Bourgogne for financial support.

[1] M. Remoissenet, *Waves Called Solitons*, 3rd ed. (Springer-Verlag, Berlin, 1999).
[2] K. E. Lonngren, *Solitons in Action*, edited by K. E. Lonngren and A. C. Scott (Academic, New York, 1978).
[3] T. B. Benjamin and J. E. Feir, J. Fluid Mech. **27**, 417 (1967).
[4] V. I. Bespalov and V. I. Talanov, Pis'ma Zh. Eksp. Teor. Fiz. **3**, 471 (1966) [JETP Lett. **3**, 307 (1966)].
[5] E. Seve, P. Tchofo Dinda, G. Millot, M. Remoissenet, J. M. Bilbault, and M. Haelterman, Phys. Rev. A **54**, 3519 (1996).
[6] T. Taniuti and H. Washimi, Phys. Rev. Lett. **21**, 209 (1968).
[7] A. Hasegawa, Phys. Rev. Lett. **24**, 1165 (1970); Phys. Fluids **15**, 870 (1971).
[8] T. Yagi and A. Noguchi, Electron. Commun. Jpn. **59**, 1 (1976).
[9] J. Sakai and T. Kawata, J. Phys. Soc. Jpn. **41**, 1819 (1976).
[10] P. Marquié, J. M. Bilbault, and M. Remoissenet, Phys. Rev. E **49**, 828 (1994).
[11] P. Marquié, J. M. Bilbault, and M. Remoissenet, Phys. Rev. E **51**, 6127 (1995).
[12] A. C. Scott, *Active and Nonlinear Wave Propagation in Electronics* (Wiley-Interscience, New York, 1970).
[13] R. Hirota and K. Suzuki, J. Phys. Soc. Jpn. **28**, 1366 (1970); Proc. IEEE **61**, 1483 (1973).
[14] H. Nagashima and Y. Amagishi, J. Phys. Soc. Jpn. **45**, 680 (1978).
[15] M. Toda, J. Phys. Soc. Jpn. **23**, 501 (1967).
[16] T. Kofané, B. Michaux, and M. Remoissenet, J. Phys. C **21**, 1395 (1988).
[17] K. Muroya, N. Saitoh, and S. Watanabe, J. Phys. Soc. Jpn. **51**, 1024 (1982).
[18] Y. Nejoh, Phys. Scr. **31**, 4185 (1985).
[19] K. B. Dysthe, Proc. R. Soc. London, Ser. A **369**, 105 (1979).
[20] M. J. Ablowitz, J. Hammack, D. Henderson, and C. M.

Schober, Phys. Rev. Lett. **84**, 887 (2000).
[21] M. J. Ablowitz, J. Hammack, D. Henderson, and C. M. Schober, Physica D **152-153**, 416 (2001).
[22] T. Taniuti and N. Yajima, J. Math. Phys. **10**, 1369 (1969).
[23] E. J. Parkes, J. Phys. A **20**, 2025 (1987).
[24] A. Hasegawa, *Optical Solitons in Fibers*, 2nd ed. (Springer-Verlag, Berlin, 1989).
[25] Y. S. Kivshar and M. Peyrard, Phys. Rev. A **46**, 3198 (1992).
[26] J. Leon and M. Manna, Phys. Rev. Lett. **83**, 2324 (1999).
[27] V. I. Karpman, Phys. Scr. **20**, 462 (1979).
[28] V. I. Karpman and V. V. Solov'ev, Physica D **1&2**, 142 (1981).
[29] T. Yagi, M. Hasegawa, and A. Noguchi, Electron. Commun. Jpn. **60**, 9 (1977).
[30] Y. Kodama and A. Hasegawa, IEEE J. Quantum Electron. **QE-23**, 510 (1987).
[31] W. Hodel and H. P. Weber, Opt. Lett. **12**, 1038 (1987).
[32] Y. Kodama and K. Nozaki, Opt. Lett. **13**, 392 (1988).
[33] F. M. Mitschke and L. F. Mollenauer, Opt. Lett. **11**, 659 (1986).
[34] J. P. Gordon, Opt. Lett. **12**, 1038 (1987).